Geol. Mag. **146** (*4*), *2009, pp. 591–601. © 2009 Cambridge University Press*
doi:10.1017/S0016756809005937 *Printed in the United Kingdom*

Interpretation of data from the monitoring thermal camera of Stromboli volcano (Aeolian Islands, Italy)

V. ZANON*†, M. NERI‡ & E. PECORA‡

*Centro de Vulcanologia e Avaliação de Riscos Geológicos, Universidade dos Açores, Rua Mãe de Deus, 9501-801 Ponta Delgada, Portugal
‡Istituto Nazionale di Geofisica e Vulcanologia, Piazza Roma, 2, I-95123 Catania, Italy

(*Received* 19 March 2008; *accepted* 20 October 2008; First published online 17 April 2009)

Abstract – Twenty eruptive events from the Northeast Crater of Stromboli volcano recorded by a thermal monitoring camera in early 2004 were analysed in order to understand the eruptive dynamics. Selected events were chosen to be typical of explosions that characterize the steady activity of Stromboli in terms of jet height and duration. Most of the explosions consisted of clast-rich single bursts, originating from the same vent inside the Northeast Crater. Conspicuous ash emission was scarce. Eruptions were preceded by the flashing of a perturbation wave characterized by low temperatures and an average propagation velocity of about 35–100 m s^{-1}. This perturbation was thought to be caused by the bursting of the gas slug at the bottom of the crater and is interpreted as an air wave. This was immediately followed by the expansion of a jet of 'hot' gas and particles, at a velocity of 35–75 m s^{-1}. Ejecta coarser than 138 cm appeared ∼1.6–2 s after the onset of the explosion, moving at a variable velocity (30–60 m s^{-1}). Eruptive events were either vertical or inclined 7–13° towards the NNW. This inclination is thought to be a consequence either of the morphology of the conduit, following modest rock falls that partially obstructed the uppermost part of the crater, or of the displacement of the internal conduit due to the explosive activity of the volcano. The instability of the summit area is a further possible cause of the deformation of the conduit.

Keywords: explosive dynamic, thermal video monitoring, volcano-tectonic structures, volcano collapses, Stromboli.

1. Introduction

The eruptive style of a volcano may change greatly with time according to several parameters, mainly linked to the instability of the volcanic edifice and to the chemical properties of erupted magmas. In this context, Strombolian activity may be only temporary and transitional phases in the eruptive history of a volcano. However, as this type of volcanic activity is characteristic of many basaltic and andesitic volcanoes of the world, during the last 30 years it has attracted the interest of many scientists who have applied different methods in an attempt to improve our understanding of the dynamics of this style of eruption.

Stromboli volcano, in the Aeolian archipelago, southern Italy, is characterized by quasi-steady activity commonly characterized by mildly explosive degassing (e.g. Rosi, Bertagnini & Landi, 2000). Any variations of this kind of activity towards more energetic forms represent a hazard for the inhabitants of the two villages along the coast and for the tourists who climb the mountain. For this reason, Stromboli has been studied since the early 1970s and, more recently, is being extensively monitored through multiparametric devices (Harris & Ripepe, 2007).

Due to the availability of a great amount of published data and the possibility to correlate them with fresh data emerging from monitoring activities, this volcano represents a suitable laboratory for the elaboration and testing of new models.

The first semi-quantitative models of Strombolian eruptions were based on the analysis of photographic images and on the study of ejecta (e.g. Chouet, Hamisevicz & McGetchin, 1974; Blackburn, Wilson & Sparks, 1976). More recent models were mainly based on the interpretation of a large amount of data produced by seismic networks, thermal and acoustic sensors installed all over the island and infrared spectroscopy of gas emissions (e.g. Vergniolle & Brandeis 1996; Vergniolle, Brandeis & Mareschal, 1996; Chouet *et al.* 1999; Ripepe & Gordeev, 1999; Johnson, 2002; McGreger & Lees, 2004; Burton *et al.* 2007).

Among these, data obtained with handheld Forward Looking Infrared Radiometer (FLIR) cameras have made it possible to develop a classification of Stromboli's mild explosive activity based on the composition and physical parameters of its jets and the velocity and duration of the events (Patrick *et al.* 2007; Patrick, 2007).

In this work, the results of a study of Stromboli's summit explosive activity, utilizing the data recorded in 2004 by a FLIR monitoring camera of the Istituto Nazionale di Geofisica e Vulcanologia installed on a flank of the volcano, are presented. The purpose is to define better the nature of the low-energy explosions, which normally characterize the activity of

†Author for correspondence: Vittorio.VZ.Zanon@azores.gov.pt

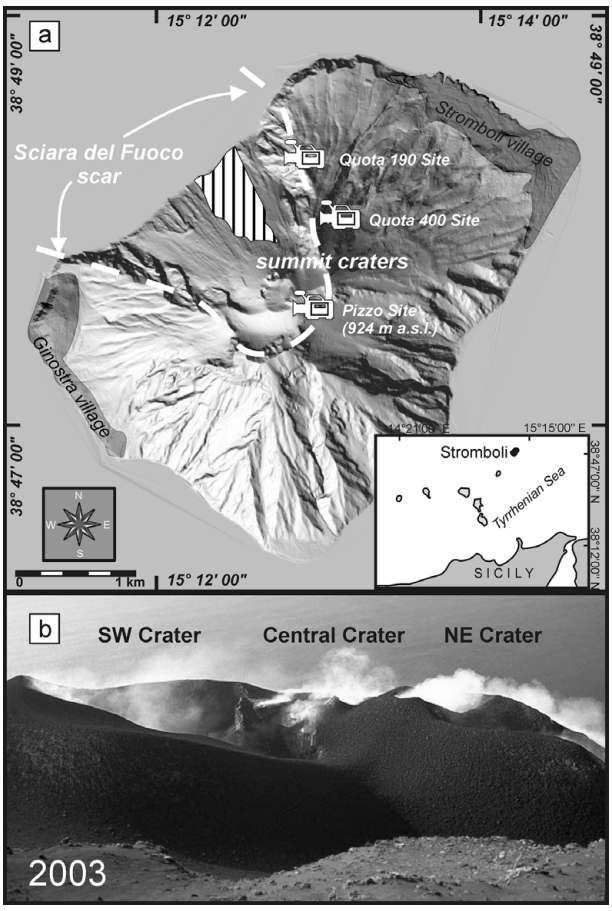

Figure 1. Digital Elevation Model of the subaerial part of Stromboli volcano (a). Among the reported morphological features there are the locations of summit craters, as well as the area affected by the 2002–2003 flank failures (striped area). The locations of the two thermal cameras (Quota 190 Site and Quota 400 Site) and of the optical camera (Pizzo Site) are shown. Summit picture (b) of the crater terrace taken from Pizzo Sopra La Fossa (924 m asl, where the optical camera is located). Fumes highlight the presence of three active craters.

this volcano, and to link their structure to some possible morphological peculiarities in the shallow conduit.

2. Geological background and recent volcanic activity

Stromboli, the northeasternmost volcano of the Aeolian Islands, rises steeply from a depth of about 2000 m on the Tyrrhenian floor, up to an elevation of 924 m above sea level (asl) (Fig. 1a). Its morphology results from an alternation of building and collapse phases, which started to occur about 100 ka ago (Gillot & Keller 1993). Several major flank failures have been recognized from the period spanning from 13 ka to AD 1350 (Pasquarè *et al.* 1993; Tibaldi, 2001; Arrighi *et al.* 2004; Apuani *et al.* 2005), consisting of landslides, which moved along a rotational sliding plane that extended below the submerged portion of the volcano.

Present-day eruptions occur from a terrace located below the top of the volcano, where there are three closely spaced active craters (Fig. 1b) with many simultaneously active vents, aligned along a zone of weakness trending NE–SW (Tibaldi, 2003). Since at least the fourth century BC (Rosi, Bertagnini & Landi, 2000), summit craters have been characterized by steady activity, which ranges from quiet degassing to low-energy Strombolian explosions, exhibiting constant volcanological and geochemical characteristics.

Low-energy Strombolian explosions are thought to be caused by the bursting of gas slugs at the top of the magma column (e.g. Jaupart & Vergniolle, 1989, Vergniolle & Brandeis, 1996). These slugs form through the collapse, at depth, of a foam made up of a collection of rising gas bubbles. While Chouet *et al.* (2003) located the slug formation area at a depth of about 220–260 m below the craters, Burton *et al.* (2007) indicated a minimum depth of about 2.7 km, in accordance with Vaggelli *et al.* (2003) and Francalanci, Tommasini & Conticelli (2004). This depth may correspond to that of a shallow reservoir where batches of magmas characterized by different gas and crystal contents mix together.

Recently, during effusive events in 2002–2003 and in 2007, steady activity at the craters stopped (Bonaccorso *et al.* 2003; Calvari *et al.* 2005; Ripepe *et al.* 2005; Falsaperla *et al.* 2006, 2008; Acocella, Neri & Scarlato, 2006). In particular, during the 2007 effusive event, dyke propagation towards the NE drained the central conduit and triggered the collapse of the shallow internal walls of the central conduit, which was previously located at about 750 m asl (Neri, Lanzafame & Acocella, 2008). Between these two effusive eruptions, and since 2007, explosive activity resumed at the summit craters, with a character which was similar to that exhibited before 2002, clearly indicating the existence of conduit peculiarities that could explain the steady activity of the volcano.

3. Methods

The present study on the dynamics of the conduit during low-energy Strombolian explosions was carried out by comparing the results emerging from the analysis of images recorded by a live monitoring camera with the morpho-structural features of the summit area.

There are three main monitoring camera sites on Stromboli volcano (http://www.ct.ingv.it/Ufso/Default.asp) (Fig. 1a). The 'Quota 190 Site' was set up in early 2007, on the northeastern rim of the Sciara del Fuoco depression, at about 190 m asl, and consists of a thermal camera. The 'Quota 400 Site', located on the same rim, but at 400 m asl, comprises both a camera operating in the visible bandwidth and a thermal camera. The last site is located on Pizzo Sopra La Fossa, where there is a second normal camera and an InfraRed (IR) camera. The summit explosions of April 2003 and March 2007 destroyed many of these devices, forcing

https://doi.org/10.1017/S0016756809005937 Published online by Cambridge University Press

the INGV to restore the damaged monitoring sites with new equipment.

We used a FLIR 320 M thermal camera that allows continuous observation of volcanic activity, both in bad weather conditions and at night, located at 'Quota 400 Site', 1042 m from the Northeast Crater, 770 m asl (Fig. 1a). It is equipped with a 320 × 240 pixel, uncooled focal plane array sensor, with a spectral range from 7.5 to 13 μm. The emissivity was fixed at 0.95 (Buongiorno, Realmuto & Doumaz, 2002). The resulting pixel size is 138 cm. Thermal sensitivity is 0.1 °C at 30 °C. The camera was set to measure temperatures in the range between 0 and 500 °C; for higher values, a 10 % error was estimated for values up to 650 °C, and a 20 % error for values from 650 to 1063 °C. The effects of atmospheric parameters (e.g. air temperature and its humidity) and the presence of volcanic gas and ash can reduce the radiation detected by the sensor of the thermal camera (Calvari & Pinkerton, 2004; Sawyer & Burton, 2006). For these reasons the recorded temperature values do not correspond to real temperatures. These data were used to evaluate instantaneous temperature variations and the development of volcanic plumes during eruptive events. Absolute temperature values were not essential.

The thermal camera is also equipped with a standard IR lens; vertical and horizontal viewing is 18° and 24°, respectively, with a spatial resolution of 1.3 mrad. A Global Positioning System time-code adds date and time to each frame. Images were stored through a time-lapse video recorder with a rate of 3.125 frames per second and digitized. Selected frames were processed with dedicated software (developed through the IMAQ Vision Builder 6.0 tool of LabVIEW^{TM}) to calculate explosion parameters (2-D parameters, area, acceleration, velocity and relative temperature) through time. To convert the number of pixels into a physical dimension, simple trigonometric calculations were performed using the known distances between video station and summit crater. Frames were captured each 0.32 s, and this means that potentially we could not detect the precise time start of events. This fact causes uncertainties on the calculation of the parameters at the beginning of the event (that is, within the first 0.32 of a second). After that moment the uncertainty is minimized.

We analysed 231 explosions from the Northeast Crater between early February and late March 2004. These events varied considerably in style and form and can be grouped in the categories described by Patrick *et al.* (2007), with a predominance of the ballistic-dominated explosions. This dataset does not include all the very low-energy explosions, in which particles hardly emerged from the crater rim, and those in which an ash plume obscured the volcanic jet, preventing any meaningful measurement. For this reason, attention was focused on 20 events, different from others in the intensity of explosions that occurred in a short period spanning from 24 to 26 February 2004. The selected events are representative of the whole dataset and of the typical activity, which characterized this period.

4. Results

A comparison of thermal images with the equivalent frames captured by the monitoring video camera operating in the range of visible wavelengths located at the same 'Quota 400 Site' provides additional information for interpreting the sequence of the images of each event. However, this camera captured images only during daylight, with a reduced resolution and at a rate of a single frame each second, thus missing many details. From this comparison, it emerged that all the explosions were fully recorded from their beginning due to the morphology of the crater area during the studied period (February 2004). The existence of a wide breach opened on the northern flank of the Northeast Crater, in fact allowed the thermal camera to record even the very first instants of each event (Fig. 2a).

Each explosion consisted of clast-rich single bursts (Fig. 2b–q) clearly separated from each other, and originating from the same vent inside the Northeast Crater. Conspicuous ash emission was scarce, appearing only at the end of each explosion. The shapes of the jets were thin in most cases, indicating that slugs were bursting at depth and that the conduit walls were controlling the direction and volume of ejecta towards the surface. In other cases, the fountain-like shape of the explosions indicated that gas bursting had occurred close to the uppermost end of the conduit. In many cases, ejecta followed fountain-like trajectories, symmetrically impacting all around the crater; in other cases, strong winds or inclined jets led to asymmetrical ejecta dispersal.

Through the processing of thermal images, it is possible to study the systematic development of single explosions in terms of the 2-D parameters of the volcanic jet, height of development of the thermal plume, and relative temperature changes (Fig. 2; Table 1).

Figure 3 shows the variations of propagation velocity of volcanic jets with time, in both vertical and horizontal directions. Propagation velocity is not uniform and it is interesting to note the existence of various velocity peaks during the developments of the jets. This makes it possible to group the explosions with similar characteristics.

In curves with only two groups of visible peaks of vertical velocity (v_v) (Fig. 3a), the first one commonly appears after 0.65 s from the beginning of the explosions, with a maximum velocity of 100 m s^{-1} and average values ranging from about 42 to 56 m s^{-1}. The second peak does not coincide with a particular instant, but it starts to appear from 1.6 to 2.23 s from the beginning of the event. Values for this second set of peaks and their shapes vary, suggesting that there is a wide range of maximum velocity values (32–65 m s^{-1}).

https://doi.org/10.1017/S0016756809005937 Published online by Cambridge University Press

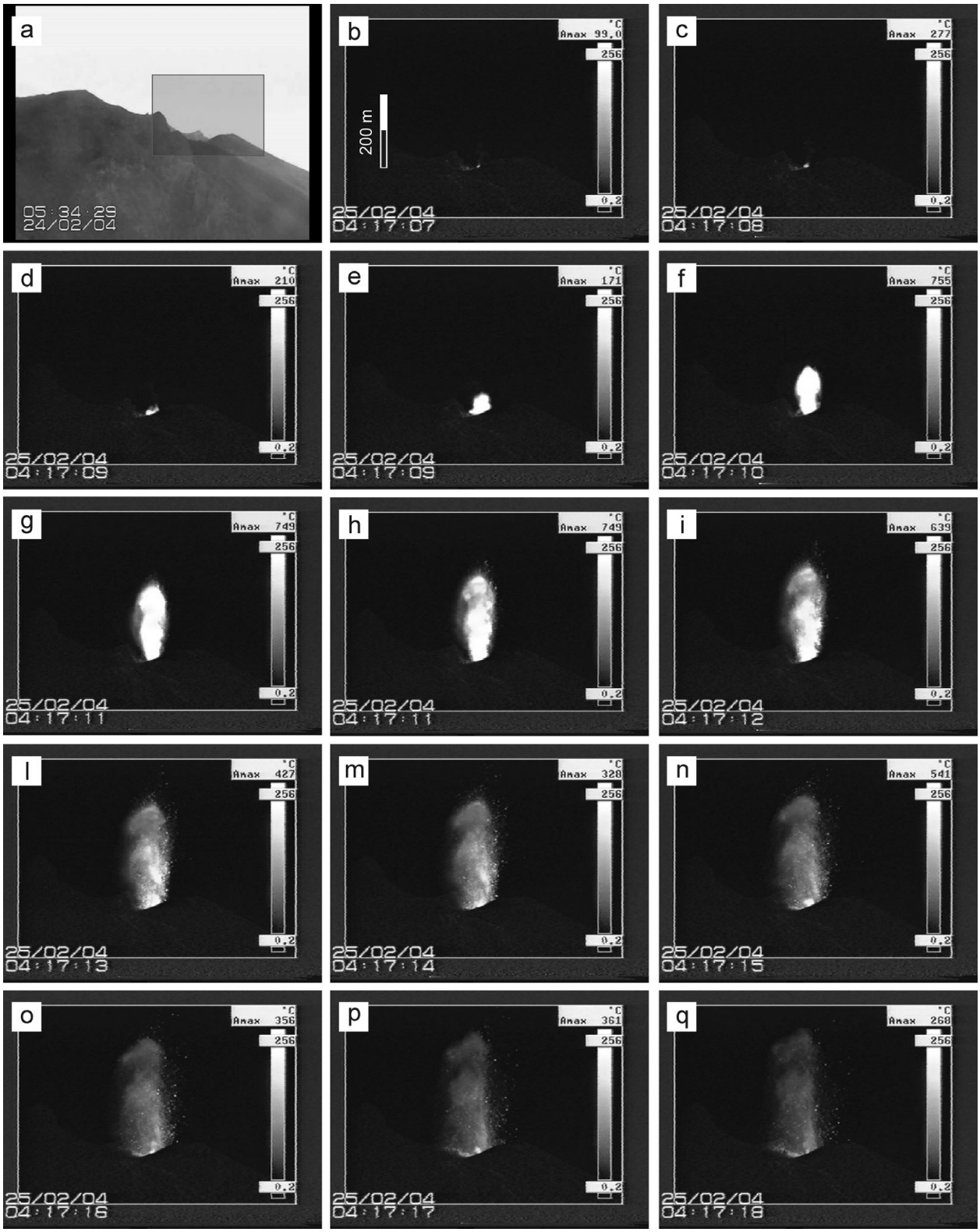

Figure 2. Selection of representative captured frames (b–q) of the explosive event which occurred on 25 February 2004 at 04:17 (GMT), recorded by the thermal camera located at 400 m asl. The scale bar is shown in (b). The thermal scale on the right-hand side is uncalibrated (see text for explanation), and shows a range of temperatures between 0.2 °C and 256 °C. Temperatures higher than 256 °C are saturated in each frame. Maximum value (Amax) indicates the highest temperature recorded by the camera. The field of view (FOV) of the thermal camera is shown in (a) with a frame recorded by the real-time camera operating in the visible bandwidth, located at the same site. Note that the morphology of the Northeast Crater was characterized in early 2004 by a wide and deep opening affecting its northern flank.

In the curves that show three groups of peaks of vertical velocity (Fig. 3b), the first developed after 0.33 s with a maximum speed of 55 m s^{-1}. The second group is made of thin peaks that formed at 0.9 s and velocities ranging between 45 and 60 m s^{-1}. The third set of peaks is slightly different for position and shape: in some

https://doi.org/10.1017/S0016756809005937 Published online by Cambridge University Press

Table 1. List of the most significant parameters measured with the FLIR thermal camera

Date (dd/mm/yy)	Beginning of explosion (hh/mm/ss/ff)	End of explosion (hh/mm/ss/ff)	v_{AW} (m s^{-1})	v_{VC} (m s^{-1})	v_{PY} (m s^{-1})	T_{AW} (°C) (1)	T_{max} (°C) (a)	Inclination (degrees) (b)
24/02/04	13.00.27.33	13.00.29.00	n.d.	60	43	48	511	7
24/02/04	13.29.13.33	13.29.14.33	55	53	28	98	611	12
24/02/04	13.42.41.00	13.42.42.00	43	n.d.	38	63	680	7
24/02/04	18.16.19.33	18.16.20.66	n.d.	68	48	47	575	7
24/02/04	21.52.46.66	21.52.47.66	60	68	60	147	693	0
24/02/04	22.30.18.33	22.30.19.33	60	40	50	188	657	6
24/02/04	23.23.26.33	23.23.27.66	55	50	38	219	634	8
25/02/04	01.35.51.66	01.35.53.00	55	63	50	123	659	6
25/02/04	02.55.56.66	02.55.58.00	n.d.	63	45	114	649	0
25/02/04	03.34.11.66	03.34.13.00	50	40	43	50	717	0
25/02/04	04.17.08.66	04.17.09.66	65	75	n.d.	210	793	0
25/02/04	04.31.25.00	04.31.26.00	n.d.	70	40	110	791	0
25/02/04	05.01.30.33	05.01.31.66	n.d.	65	53	n.d.	741	0
25/02/04	06.07.39.33	06.07.40.66	n.d.	113	n.d.	204	698	0
25/02/04	07.47.45.33	07.47.46.66	60	55	58	53	689	0
25/02/04	09.50.12.66	09.50.14.33	60	65	n.d.	118	756	0
25/02/04	12.26.09.66	12.26.11.00	63	55	n.d.	114	725	7
25/02/04	16.02.10.66	16.02.12.66	40	43	28	77	639	0
26/02/04	14.50.43.66	14.50.45.33	60	n.d.	n.d.	49	744	0
26/02/04	18.42.44.33	18.42.45.66	53	63	n.d.	50	527	6

Abbreviations: v_{AW} – velocity of air wave; v_{VC} – vertical velocity of expansion of volcanic jet; v_{PY} – vertical velocity of late stage ejecta, larger than 138 cm; T_{AW} – temperature of air wave; T_{max} – maximum temperature of the volcanic jet. Timing is GMT.
Note (a): the scale of temperature values is not calibrated. Note (b): the inclination of the conduit is measured towards the NW in respect of the azimuth.

curves it shows up 1.62–3.2 s after the start of the event; the peaks have a thin shape and maximum velocity of 52 m s^{-1}. It seems that there is no relationship among the velocities of the different groups of peaks.

During the analysis of each frame, the instant horizontal velocity (v_h) of the expansion of the volcanic jets was measured from the moment of first detection. The 75 % of the curves of the v_h consistently shows up 0.32 s after the onset of the explosion (Fig. 3c). It is clearly separated from the other peaks and its velocity ranges between 17 and 38 m s^{-1}. Afterwards, curves of v_h show irregular paths with randomly distributed peaks and values, on average, ranging from 10 to 2.5 m s^{-1}. In general, lateral expansion of volcanic plumes seems to be inhomogeneous and develops in small impulses. In the remaining 25 % of the curves (Fig. 3d), the shape of the first group of velocity peaks is broader, and these peaks develop about 0.6 s after the onset of the event with an average velocity of 15 m s^{-1} (with a single case of 25 m s^{-1}). After about 1.6 s, a second group develops, characterized by smaller velocities (not exceeding 8 m s^{-1}, with a single exception of 37 m s^{-1}). After these peaks, the velocity signal is not clear even where a third peak seems to become evident.

By comparison with data reported in Patrick (2007), obtained recording thermal images at a shorter distance and using a higher ratio frame/second, we obtained the same values of vertical velocity and, on average, a slightly higher velocity of lateral plume spreading (> 4 m s^{-1}), with important spikes. This discrepancy could be related to the fact that we did not use any filtering option in order to observe any possible variation.

The thermal plume carries the smallest particles and gas at variable velocity (Fig. 4a). The rate of velocity decrease is about the same for all the curves; after 6.1 s, plots indicate that plume rise is over. During this phase, the persistence of volcanic material at heights of 100–160 m is therefore only related to the buoyancy of the plume. The maximum heights reached by volcanic plumes changed by more than 60 m during the period under study. There is no relationship between the maximum heights reached by these plumes and the change in atmospheric conditions (air temperature, mainly) from day to night. This means that the maximum heights reached are strictly dependent on the physical characteristics of each single explosion.

The diagram of relative temperature values (T) (Fig. 4b) reveals the development of a small but clear peak that developed immediately after 0.32 s, characterized by low values. After 0.98 s, there is an abrupt rise in values, which constitutes the second and main peak of temperatures. These values exceed those of the first peak by a factor of four. After this second peak, values remain constant, on average, up to 2.6 s after the beginning of the event. During this phase, the plume expands and starts to cool down. The rate of cooling is the same for all the explosions.

About 50 % of the volcanic jets studied from video images are vertical with respect to the focal plane of the camera, while the other jets dip towards the NW by 7–13° regardless of wind direction. These explosions have a compact shape and last for a couple of seconds, while the shape of vertical jets is soon deformed by the lateral expansion of gases. It appears that there is

https://doi.org/10.1017/S0016756809005937 Published online by Cambridge University Press

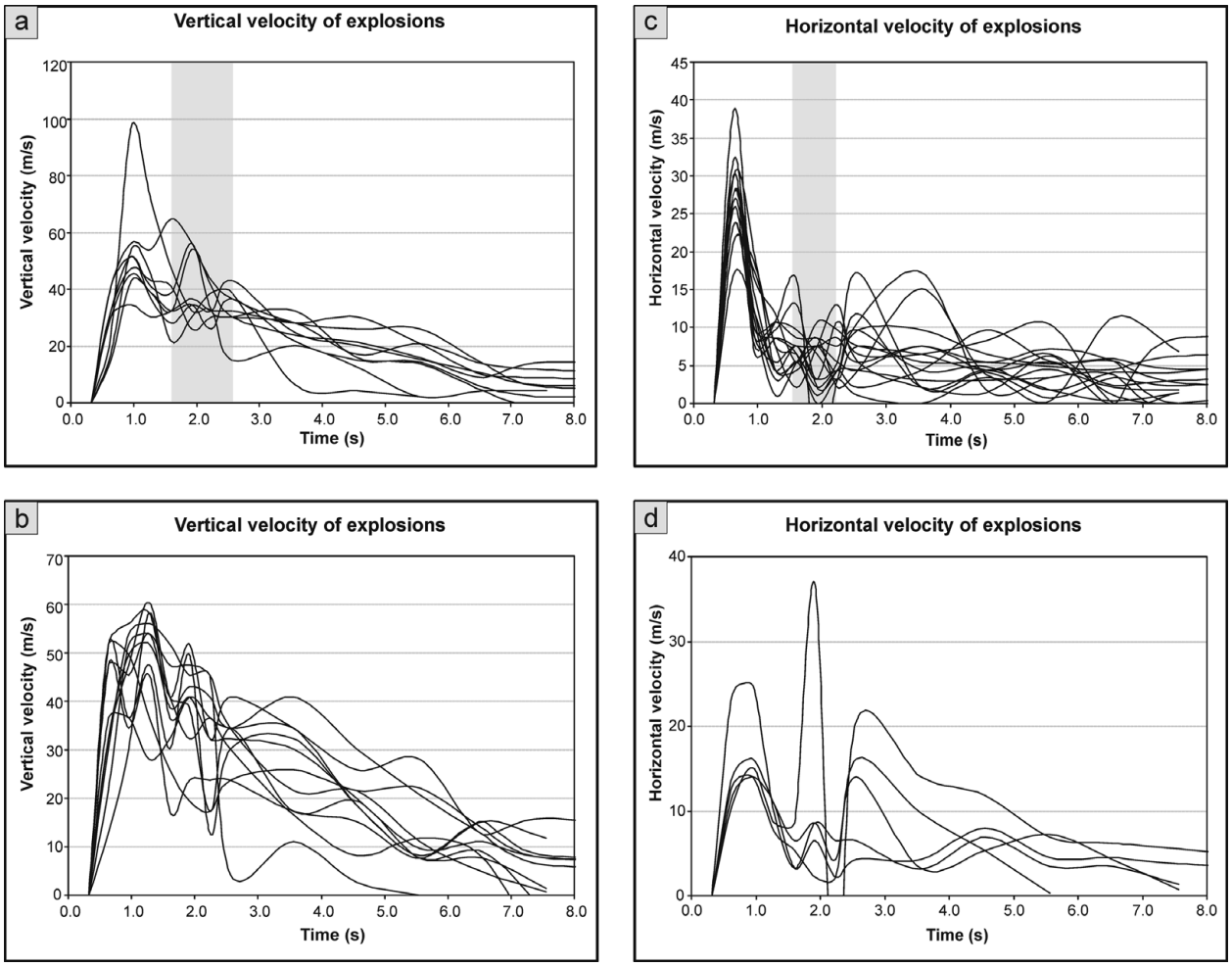

Figure 3. Plots of velocity data emerging from the analysis of video recordings from the thermal camera. Plots are distinguished based on the number of populations of peaks and their temporal distribution during the development of the eruptive events. In (a) and (b) the variations of the vertical velocity of the volcanic jet (v_v) are plotted versus time. In (a) the first set of peaks is coaxial but characterized by large variations of velocity; the following peaks are not coaxial (represented with the grey area) and show a reduced variation of velocity. In (b) there are three sets of peaks that are all coaxial with comparable variations in velocity. In (c) and (d) the variations of the vertical velocity of the volcanic jet (v_h) are reported versus time.

no relationship between inclination, exit velocity, and volume of the jets.

5. Discussion

The interpretation of the images captured by the monitoring thermal camera of the INGV, which is working at a long distance from the Northeast Crater of the volcano, provides useful semi-quantitative information for understanding the explosive dynamics of the volcano. Some major approximations and errors, however, prevent us from applying these conclusions to all Strombolian events.

Before any interpretation of these results, it is important to remember that they emerged from a flux analysis of semi-continuous data recorded at a 0.32 s interval. The large amount of data collected partially compensates for the low resolution of the sensor, caused by the long recording distance.

Secondly, it should be considered that changing conduit morphology may cause changes in the eruptive style. Erosion, partial failure of inner walls and fracturing due to gas bursting can occur during the lifetime of a feeder conduit, affecting the morphology of craters and, subsequently, the style of eruptions.

The major limitation to this model is the pixel size of 138 cm. This value is higher than that calculated by Patrick *et al.* (2007), since these authors used a hand-held thermal camera and viewed the craters from a reduced distance (450 m or less). As most of the ejecta emitted during a single blast at Stromboli volcano is in the range of 30–120 cm (e.g. Chouet, Hamisevicz & McGetchin, 1974; Ripepe, Rossi & Saccorotti, 1993; Hort, Seyfried & Voge, 2003), considerations on the genesis of Strombolian events are therefore meaningless. However, notwithstanding this limitation, some new interesting features can be outlined.

5.a. Interpretation of observed features and eruptive dynamics

The most interesting results are obtained from the analysis of the plots in Figures 3 and 4, where the velocity values constantly show a peak at 0.66 s after the

https://doi.org/10.1017/S0016756809005937 Published online by Cambridge University Press

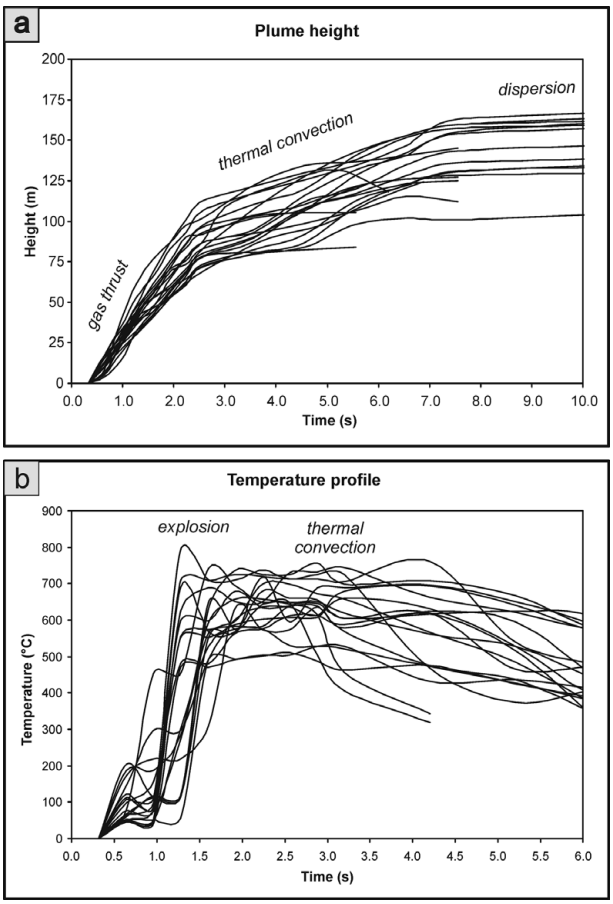

Figure 4. Developments of explosions in terms of stages of ascent. Curves in (a) indicate the instant cumulative heights of the volcanic jets and show how the ascent of the plume is initially due to the gas thrust phase, first followed by the thermal ascent of gas and fine ejecta, and lastly, by the dispersion operated by winds. In (b) the peaks of instant maximum temperature are reported. These curves are produced utilizing each single maximum value of temperature recorded by the sensor in any frame and reported in the upper right-hand side.

beginning of the explosive events. A contemporaneous variation of temperature is also apparently associated with this velocity peak.

In order to interpret these phenomena, it is necessary to consider the results of the modelling of infrasound signals recorded in various periods near the crater terrace, and to compare them with those emerging from equivalent fieldwork on other volcanoes characterized by similar behaviour (e.g. Braun & Ripepe, 1993; Vergniolle & Brandeis, 1994; Johnson 2002; McGreger & Lees, 2004).

On Stromboli, acoustic waveforms start with an impulsive couplet comprising a compressional signal, followed by decompression (10 ± 4 Pa: McGreger & Lees, 2004; Vergniolle & Brandeis, 1994). This signal is contemporaneous with the occurrence of the peak observed in Figures 3 and 4, even though, due to the difference between the velocity propagation of light and that of acoustic waveforms, there is a consequent time scattering.

The existence of this couplet has also been observed during minor explosive eruptions at other volcanoes,

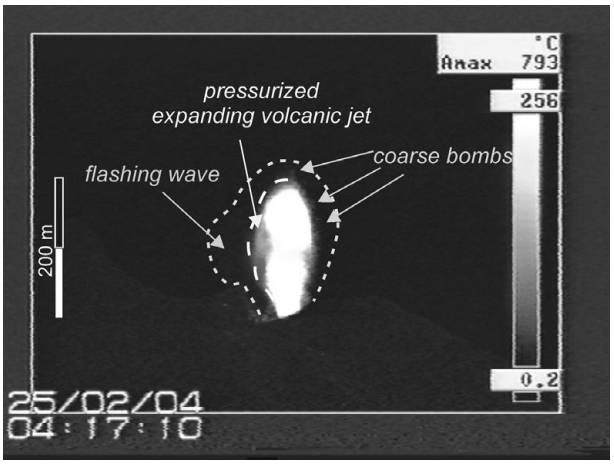

Figure 5. Constitution of a typical explosion, after interpretation of the peaks of velocities, indicated by the analysis of thermal images. The flashing wave precedes the expansion of the main volcanic jet and the ejection of bombs coarser than 138 cm.

and was interpreted either as the sound produced by bubbles vibrating on the magma-free surface (Vergniolle & Brandeis, 1994; Vergniolle, Brandeis & Mareschal, 1996) or by rapid gas expansion outside the vent after the explosion of the bubbles (Braun & Ripepe, 1993; Firstov & Kravchenko, 1996; Vergniolle, Brandeis & Mareschal, 1996; Rowe *et al.* 2000; Johnson & Lees, 2000; Johnson, Aster & Kyle, 2004).

As the peaks shown in Figures 3 and 4 can neither represent sound (since their propagation velocity is much less than that of sound) nor a perturbation produced by the arrivals of P-seismic waves at the soil–air boundary (the halo is observed only around the volcanic jet and not around the profile of the crater), they should be interpreted as air perturbation linked to the eruptive jet.

The rapid release of pressurized gas during the burst of a gas slug prompts an air wave (e.g. Braun & Ripepe, 1993; Johnson, 2002), which propagates above the crater and precedes the development of the main volcanic jet. The thermal peak shown in Figure 4 may be explained by the sudden compression and decompression of the plume mixture crossed by the wave. This flashing air wave is evident in Figure 5, where a low-temperature halo, enveloping the eruptive jet and lasting only a few fractions of a second, is shown. When the air wave reaches the crater rim, it initiates a rapid lateral expansion, moving horizontally, at a velocity that is, on average, twice that of the volcanic jet. This phenomenon is thought to be always present, but it was evident only in the most powerful explosions showing a vertical blast. On the contrary, it was not observed in low fountain-like explosions.

The presence of an air wave during explosive events has been reported during observations of Vulcanian explosions (e.g. Perret, 1912; Nairn, 1976; Livshits & Bolkhovitinov, 1977; Yokoo, Ichihara & Taniguchi, 2004; Yokoo & Taniguchi, 2004), but not previously reported from Strombolian-type explosions.

https://doi.org/10.1017/S0016756809005937 Published online by Cambridge University Press

A few ideas can be put forward as to the nature of the other peaks shown in Figures 3 and 4, in the absence of synchronized high-resolution visible images. To be cautious it may be noted that the flashing wave is always soon followed by the expansion of a dense cloud of magmatic gases and quite small (< 138 cm) incandescent ejecta, which constitute most of the visible erupted material. The velocity values measured for the eruptive jets are in agreement with those reported by Chouet, Hamisevicz & McGetchin (1974); Blackburn, Wilson & Sparks (1976); Weill *et al.* (1992); Ripepe, Rossi & Saccorotti (1993), Ripepe, Ciliberto & Della Schiava (2001); Ripepe (1996); Hort & Seyfried (1998); Hort, Seyfried & Voge (2003); Patrick (2007) and Patrick *et al.* (2007).

Ejecta of an appreciable size (> 138 cm) become visible only after 1.5 s after the onset of the event (Fig. 2g–q). The ejection of this coarse material can last for a few seconds, forming something like a very small-volume lava fountain. The presence of large hot bombs cannot be excluded during the first development phases of an eruptive jet, due to the high density of the particles contained in it. Single clasts reach heights that are comparable with those of the mass erupted some instants before.

The material hurled from the vent, considered as a whole, becomes buoyant at a height between 70 and 115 m, commonly 2 seconds (s) after emission from the conduit.

Once the maximum height allowed by the kinetic energy of the explosion is reached, the volcanic mixture remains stable for a few fractions of a second, and then starts to expand laterally and to rise, because of the development of thermals above the crater (Fig. 4a).

5.b. Modelling of the ascent in upper conduit and the eruptions

The minimum diameter of the base of the volcanic jets from our observations was calculated to be about 6–8 m, in agreement with direct visual observations and with measurements from the helicopter during monitoring activities.

Nine out of twenty jets dip ∼7–13° towards the NW, regardless of wind direction. In the other cases, vertical explosions were observed. These were likely generated by gas slugs bursting on the surface of a magmatic column whose free surface is very close to the base of the vent. In this case, volcanic jets were not deflected by the conduit walls and could expand freely, generating vertical, fountain-like explosions, with pyroclasts falling symmetrically around the crater.

Inclined jets could be generated by deep-seated slug bursts in an inclined conduit. In this case, the shape of these jets may be constrained by the conduit walls, and pyroclasts are ejected towards the steep slope of the Sciara del Fuoco.

In the images taken by the optical monitoring camera located at Pizzo Sopra La Fossa, the same inclined explosions recorded by the IR camera appear to be vertical. However, although the FLIR thermal camera

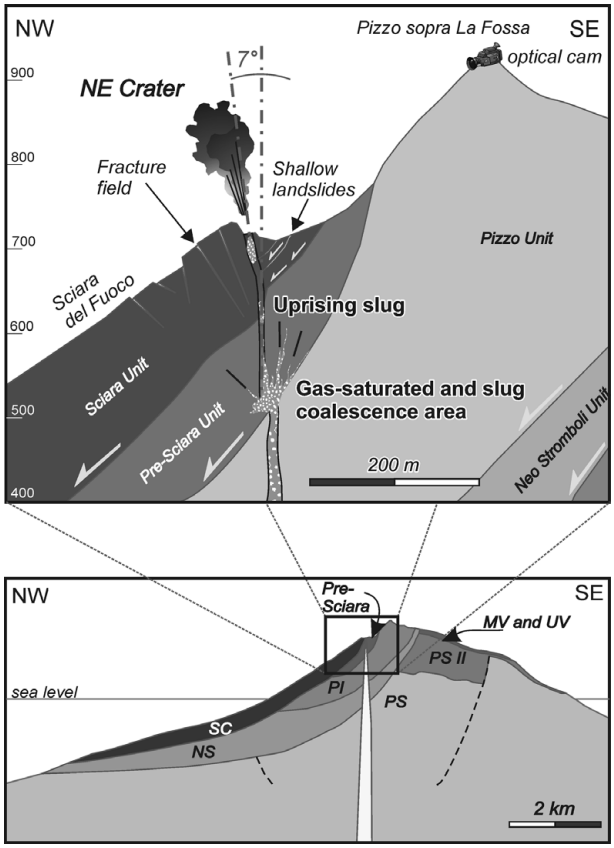

Figure 6. Section of the emerged part of Stromboli volcano, redrawn after Apuani *et al.* (2005) and the model of its inner structure with the displacement of the shallower section of Northeast Crater conduit. Abbreviations are as follows: PS – Paleostromboli unit; PS II – Paleostromboli II unit; NS – Neostromboli unit; PI – Pizzo Unit; SC – Sciara Unit; MV – Middle Vancori; UV – Upper Vancori. The shallow landslides affecting the volcanic deposits located between the summit craters and Pizzo Sopra la Fossa might significantly contribute to the inclination of some volcanic jets. See the text for further details.

captures a lateral view of the eruptive vent, it is located in an almost orthogonal position with respect to the optical camera (Fig. 1a) and for this reason the recorded inclination of the eruptive jets is considered to represent the true value. On the other hand, the inclination of jets might also be due to the morphology of the shallow conduit that undergoes continuous remodelling after each explosion.

The same inclination of the Strombolian jets is evident in some images published by Patrick *et al.* (2007). These features could be explained by the seaward inclination of the conduit in its upper segment, which might be linked to the sliding movement affecting the Sciara Unit (Fig. 6). Indeed, the volcanic material constituting the two youngest depositional units of Stromboli (Pre-Sciara and Sciara units) has undergone a series of differential displacements (Arrighi *et al.* 2004; Apuani *et al.* 2005) (Fig. 6). Starting from $< 5.6 \pm 3.3$ ka (Gillot & Keller, 1993), the Pre-Sciara Unit, made up mainly of lava flows, probably underwent a small rotational slump in the area below the craters. Such a displacement might have

https://doi.org/10.1017/S0016756809005937 Published online by Cambridge University Press

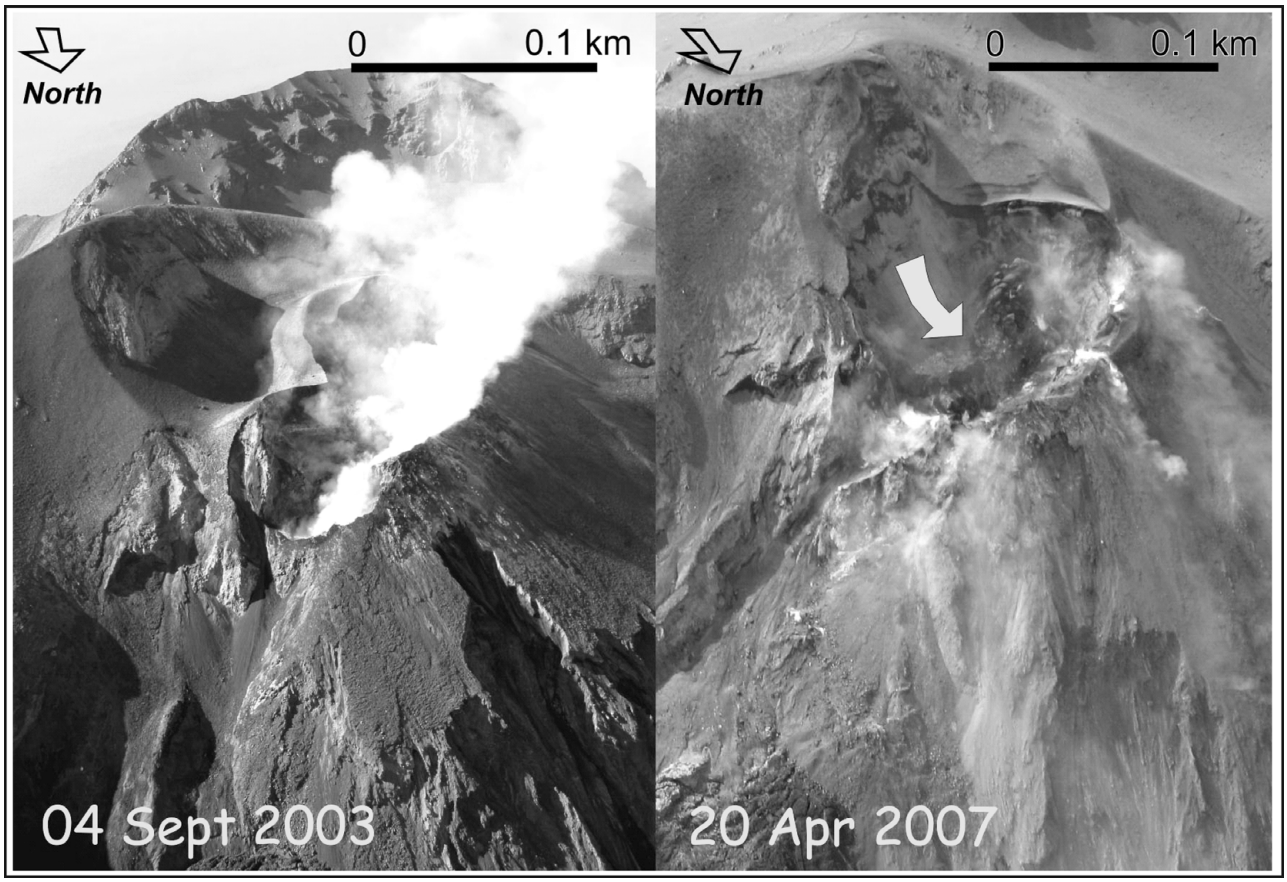

Figure 7. The summit craters of Stromboli in 2003 and in 2007. The area located between Pizzo Sopra la Fossa and the summit crater terrace collapsed into the conduit (grey arrow) during the 2007 eruption, revealing the geometry of the walls of the conduit at shallow depth.

caused the displacement of the feeding system with the formation of a sort of siphon, probably located 220–260 m below the craters, along the sliding plane. The presence of this siphon, as suggested by Ballestracci (1982), hinders the normal ascent rate of gas pockets from depth, playing a role in the regularity of the summit activity of Stromboli.

A second more feasible explanation envisages the inclination of the very shallow portion of the conduit (a few tens of metres) related to small-volume landslides and rockfalls into the crater terrace below Pizzo Sopra la Fossa (Fig. 6). These events are triggered by both the seismic activity that accompanies the explosive activity and by the collapse of the Northeast Crater walls due to the height variation of the magma column free surface inside the conduits. This process was highlighted during the 2007 eruption (Neri, Lanzafame & Acocella, 2008), when continuous obstruction of the crater forced ascending magma to find a way out where principal stresses offered the minimum resistance, that is, towards the NW. As a result, the uppermost segment of the conduit is characterized by asymmetric walls (Fig. 7) which can deviate and bow the volcanic jets generated by the explosions.

6. Concluding remarks

Stromboli volcano is one of the main concerns of Italian Civil Protection, due to the proximity of urbanized areas to the craters and the numerous tourists who climb the volcano every day. Continuous monitoring of its activity is of fundamental importance for the safety of the inhabitants of the island and for the application of innovative methodologies to comprehend eruptive mechanisms. Installation of surveillance devices is one of the greatest efforts of the scientific community. After the violent explosions of 5 April 2003 and 15 March 2007, the damaged or destroyed monitoring network on the island was completely substituted with new equipment, which is providing new data of better quality.

This study, based on images of a series of low-energy Strombolian explosions from the Northeast Crater, captured by the thermal monitoring camera, provides new information about the dynamics of Strombolian activity and the role of the conduit morphology and the summit instability.

The careful observation of sequences of explosions has made it possible to outline some features of Strombolian explosions. In particular, it was evident that a perturbation is visible for a few fractions of a second after the generation of the volcanic jet. Similar perturbations had been captured in the past by high-speed shutter cameras during great explosive events (mostly Vulcanian) in other volcanoes, and interpreted as air waves. Their presence during Strombolian eruptions was only hypothesized after the application of other geophysical methodologies but they were never detected.

https://doi.org/10.1017/S0016756809005937 Published online by Cambridge University Press

By integrating these data with the results achieved by other authors, it was demonstrated that summit instability could play an important role in the present geometry of the conduit of the Northeast Crater and in the constant and rhythmic occurrence of explosions at Stromboli volcano since the fourth century BC. The morphology of the upper segment of the conduit appears to be affected by continuous remodelling, which could be the reason for the temporary seaward inclination by tens of metres of the shallow portion of the conduit itself. This inclination could be also related to the sliding movement of the Sciara del Fuoco and/or to the small-scale landslides (rockfalls) that involve the area located immediately below the Pizzo Sopra la Fossa and that subsequently fall into the crater.

Acknowledgements. This work was partially funded by the Istituto Nazionale di Geofisica e Vulcanologia and the Dipartimento della Protezione Civile, Italy, project INGV-DPC V2. Letizia Spampinato, Alessandro Tibaldi, Nicole Lautze and Matthew Patrick are gratefully acknowledged for their useful suggestions to develop this work. Thanks are also extended to Boris Behncke for his helpful discussion on the dynamics of the Strombolian activity and to Steve Conway for improving the English language of the manuscript.

References

ACOCELLA, V., NERI, M. & SCARLATO, P. 2006. Understanding shallow magma emplacement at volcanoes: Orthogonal feeder dykes during the 2002–2003 Stromboli (Italy) eruption. *Geophysical Research Letters* **33**(17), L17310, doi:10.1029/2006GL026862.

APUANI, T., CORAZZATO, C., CANCELLI, A. & TIBALDI, A. 2005. Stability of a collapsing volcano (Stromboli, Italy): Limit equilibrium analysis and numerical modelling. *Journal of Volcanology and Geothermal Research* **144**, 191–210.

ARRIGHI, S., ROSI, M., TANGUY, J. C. & COURTILLOT, V. 2004. Recent eruptive history of Stromboli (Aeolian Islands, Italy) determined from high-accuracy archeomagnetic dating. *Geophysical Research Letters* **31**(L19603), doi:10.1029/2004GL020627.

BALLESTRACCI, R. 1982. Self-potential survey near the craters of Stromboli volcano (Italy). Inference for internal structure and eruption mechanism. *Bulletin of Volcanology* **45**(4), 349–65.

BLACKBURN, E. A., WILSON, L. & SPARKS, R. S. J. 1976. Mechanisms and dynamics of strombolian activity. *Journal of the Geological Society, London* **132**, 429–40.

BONACCORSO, A., CALVARI, S., GARFÌ, G., LODATO, L. & PATANE, D. 2003. Dynamics of the December 2003 flank failure and tsunami at Stromboli volcano inferred by volcanological and geophysical observations. *Geophysical Research Letters* **30**(18), 1941–4.

BRAUN, T. & RIPEPE, M. 1993. Interaction of seismic and air waves recorded on Stromboli Volcano. *Geophysical Research Letters* **20**(1), 65–8.

BUONGIORNO, M. F., REALMUTO, V. J. & DOUMAZ, F. 2002. Recovery of spectral emissivity from thermal infrared multispectral scanner imagery acquired over a mountainous terrain: A case study from Mount Etna Sicily. *Remote Sensing of Environment* **79**, 123–33.

BURTON, M. R., ALLARD, P., MURÈ, F. & LA SPINA, A. 2007. Magmatic gas composition reveals the source depth of slug-driven Strombolian explosive activity. *Science* **317**, 227–30.

CALVARI, S. & PINKERTON, H. 2004. Birth, growth and morphologic evolution of the 'Laghetto' cinder cone during the 2001 Etna eruption. *Journal of Volcanology and Geothermal Research* **132**(2–3), 225–39.

CALVARI, S., SPAMPINATO, L., LODATO, L., HARRIS, A. J. L., PATRICK, M. R., DEHN, J., BURTON, M. R. & ANDRONICO, D. 2005. Chronology and complex volcanic processes during the 2002–2003 flank eruption at Stromboli volcano (Italy) reconstructed from direct observations and surveys with a handheld thermal camera. *Journal of Geophysical Research* **110**, B02201, doi:10.1029/2004JB003129.

CHOUET, B., DAWSON, P., OHMINATO, T., MARTINI, M., SACCOROTTI, G., GIUDICEPIETRO, F., DE LUCA, G., MILANA, G. & SCARPA, R. 2003. Source mechanisms of explosions at Stromboli volcano, Italy, determined from moment-tensor inversions of very-long-period data. *Journal of Geophysical Research* **108**(B1), 2019, doi:10.1029/2002JB001919.

CHOUET, B., HAMISEVICZ, N. & MCGETCHIN, T. R. 1974. Photoballistics of volcanic jet activity at Stromboli, Italy. *Journal of Geophysical Research* **79**, 4961–76.

CHOUET, B., SACCOROTTI, G., MARINI, M., DAWSON, P., DE LUCA, G., MILANA, G., CATTANEO, M. & SCARPA, R. 1999. Source and path effects in the wave fields of tremor and explosions at Stromboli Volcano, Italy. *Geophysical Research Letters* **29**, 1937–40.

FALSAPERLA, S., MAIOLINO, V., SPAMPINATO, S., JAQUET, O. & NERI, M. 2008. Sliding episodes during the 2002–2003 Stromboli lava effusion: insights from seismic, volcanic, and statistical data analysis. *Geochemistry, Geophysics, Geosystems* **9**, Q04022, doi:10.1029/2007GC001859.

FALSAPERLA, S., NERI, M., PECORA, E. & SPAMPINATO, S. 2006. Multidisciplinary study of flank instability phenomena at Stromboli volcano, Italy. *Geophysical Research Letters* **33**, L09304, doi:10.1029/2006GL025940.

FIRSTOV, P. P. & KRAVCHENKO, N. M. 1996. Estimation of the amount of explosive gas released in volcanic eruptions using air waves. *Vulkanologiya i Seismologiya* **17**, 547–60.

FRANCALANCI, L., TOMMASINI, S. & CONTICELLI, S. 2004. The volcanic activity of Stromboli in the 1906–1998 AD period: mineralogical, geochemical and isotope data relevant to the understanding of the plumbing system. *Journal of Volcanology and Geothermal Research* **131**(1–2), 179–211.

GILLOT, P. Y. & KELLER, J. 1993. Radiochronological dating of Stromboli. *Acta Vulcanologica* **3**, 69–77.

HARRIS, A. J. L. & RIPEPE, M. 2007. Synergy of multiple geophysical approaches to unravel explosive eruption conduit and source dynamics – A case study from Stromboli. *Chemie der Erde* **67**, 1–35.

HORT, M. & SEYFRIED, R. 1998. Volcanic eruption velocities measured with a micro radar. *Geophysical Research Letters* **25**(1), 113–16.

HORT, M., SEYFRIED, R. & VOGE, M. 2003. Radar Doppler velocimetry of volcanic eruptions: theoretical considerations and quantitative documentation of changes in eruptive behavior at Stromboli volcano, Italy. *Geophysical Journal International* **154**, 515–32.

JAUPART, C. & VERGNIOLLE, S. 1989. The generation and collapse of a foam layer at the roof of a basaltic magma chamber. *Journal of Fluid Mechanics* **203**, 347–80.

JOHNSON, J. B. 2002. Generation and propagation of infrasonic airwaves from volcanic explosions. *Journal of Volcanology and Geothermal Research* **121**, 1–14.

JOHNSON, J. B., ASTER, R. C. & KYLE, P. R. 2004. Volcanic eruptions observed with infrasound. *Geophysical Research Letters* **31** (L14604), doi:10.1029/2004GL020020.

JOHNSON, J. B. & LEES, J. M. 2000. Plugs and chugs – seismic and acoustic observations of degassing explosions at Karymsky, Russia and Sangay, Ecuador. *Journal of Volcanology and Geothermal Research* **101**(1–2), 67–82.

LIVSHITS, L. D. & BOLKHOVITINOV, L. G. 1977. Weak shock waves in the eruption column. *Nature* **267**, 420–1.

MCGREGER, A. D. & LEES, J. M. 2004. Vent discrimination at Stromboli Volcano, Italy. *Journal of Volcanology and Geothermal Research* **137**, 169–85.

NAIRN, I. A. 1976. Atmospheric shock waves and condensation clouds from Ngauruhoe explosion eruption. *Nature* **259**, 190–2.

NERI, M., LANZAFAME, G. & ACOCELLA, V. 2008. Dike emplacement and related hazard in volcanoes with sector collapse: the 2007 Stromboli eruption. *Journal of the Geological Society, London* **165**, 883–6.

PASQUARÈ, G., FRANCALANCI, L., GARDUÑO, V. H. & TIBALDI, A. 1993. Structure and geological evolution of the Stromboli volcano, Aeolian Islands, Italy. *Acta Vulcanologica* **3**, 79–89.

PATRICK, M. R. 2007. Dynamics of Strombolian ash plumes from thermal video: motion, morphology, and air entrainment. *Journal of Geophysical Research* **112** (B06202), doi:10.1029/2006JB004387.

PATRICK, M. R., HARRIS, A. J. L., RIPEPE, M., DEHN, J., ROTHERY, D. A. & CALVARI, S. 2007. Strombolian explosive styles and source conditions: insights from thermal (FLIR) video. *Bulletin of Volcanology* **69**(7), 769–84.

PERRET, A. F. 1912. The flashing arcs: A volcanic phenomenon. *American Journal of Science* **4**, 329–33.

RIPEPE, M. 1996. Evidence for gas influence on volcanic seismic signals recorded at Stromboli. *Journal of Volcanology and Geothermal Research* **70**(3–4), 221–33.

RIPEPE, M., CILIBERTO, S. & Della SCHIAVA, M. 2001. Time constraint for modelling source dynamics of volcanic explosions at Stromboli. *Journal of Geophysical Research* **106**, 8713–27.

RIPEPE, M. & GORDEEV, E. 1999. Gas bubble dynamics model for shallow volcanic tremor at Stromboli. *Journal of Geophysical Research* **104**(B5), 10639–54.

RIPEPE, M., MARCHETTI, E., ULIVIERI, G., HARRIS, A. J. L., DEHN, J., BURTON, M., CALTABIANO, T. & SALERNO, G. 2005. Effusive to explosive transition during the 2003 eruption of Stromboli volcano. *Geology* **33**(5), 341–4.

RIPEPE, M., ROSSI, M. & SACCOROTTI, G. 1993. Image processing of explosive activity at Stromboli. *Journal of Volcanology and Geothermal Research* **54**(3–4), 335–51.

ROSI, M., BERTAGNINI, A. & LANDI, P. 2000. Onset of the persistent activity at Stromboli Volcano (Italy). *Bulletin of Volcanology* **62**, 294–300.

ROWE, C. A., ASTER, R. C., KYLE, P. R., DIBBLE, R. R. & SCHLUE, J. W. 2000. Seismic and acoustic observations at Mount Erebus Volcano, Ross Island, Antarctica, 1994–1998. *Journal of Volcanology and Geothermal Research* **101**, 105–28.

SAWYER, G. M. & BURTON, M. R. 2006. Effects of a volcanic plume on thermal imaging data. *Geophysical Research Letters* **33**(14), doi:10.1029/2005GL025320.

TIBALDI, A. 2001. Multiple sector collapses at Stromboli volcano, Italy: How they work. *Bulletin of Volcanology* **63**(2–3), 112–25.

TIBALDI, A. 2003. Influence of cone morphology on dykes, Stromboli, Italy. *Journal of Volcanology and Geothermal Research* **126**, 79–95.

VAGGELLI, G., FRANCALANCI, L., RUGGIERI, G. & TESTI, S. 2003. Persistent polybaric rests of calc-alkaline magmas at Stromboli volcano, Italy: pressure data from fluid inclusions in restitic quartzite nodules. *Bulletin of Volcanology* **65**(6), 385–404.

VERGNIOLLE, S. & BRANDEIS, G. 1994. Origin of the sound generated by Strombolian explosions. *Geophysical Research Letters* **21**(18), 1959–62.

VERGNIOLLE, S. & BRANDEIS, G. 1996. Strombolian explosions, 1, A large bubble breaking at the surface of a lava column as a source of sound. *Journal of Geophysical Research* **101**(B9), 20433–48.

VERGNIOLLE, S., BRANDEIS, G. & MARESCHAL, J. C. 1996. Strombolian explosions, 2, Eruption dynamics determined from acoustic measurements. *Journal of Geophysical Research* **101**(B9), 20449–66.

WEILL, A., BRANDEIS, G., VERGNIOLLE, S., BAUDIN, F., BILBILLE, J., FÉVRE, J. F., PIRON, B. & HILL, X. 1992. Acoustic sounder measurements of the vertical velocity of volcanic jets at Stromboli volcano. *Geophysical Research Letters* **19**(23), 2357–60.

YOKOO, A., ICHIHARA, M. & TANIGUCHI, H. 2004. Flashing arc on Izu–Oshima 1986 eruption. *Bulletin of the Volcanological Society of Japan* **49**, 299–304.

YOKOO, A. & TANIGUCHI, H. 2004. Application of video image processing to detect volcanic pressure waves: A case study on archived images of Aso Volcano, Japan. *Geophysical Research Letters* **31**(23), L23604.